# MEASURING ULTRASONIC CHARACTERISATION TO DETERMINE THE IMPACT OF TOC AND THE STRESS FIELD ON SHALE GAS ANISOTROPY

*Lead author*
**Yazeed Altowairqi**

**Y. Altowairqi[1], R. Rezaee[1], M. Urosevic[2] and C. Delle Piane[3]**
[1]Department of Petroleum Engineering
Level 6 ARRC Building, Curtin University
26 Dick Perry Avenue
Kensington WA 6151
[2]Department of Geophysics
Level 4 ARRC Building, Curtin University
26 Dick Perry Avenue
Kensington WA 6151
[3]CSIRO
Level 2 ARRC Building, Curtin University
26 Dick Perry Avenue
Kensington WA 6151
y.altowairqi@postgrad.curtin.edu.au

## ABSTRACT

**While the majority of natural gas is produced from conventional sources, there is significant growth from unconventional sources, including shale-gas reservoirs. To produce gas economically, candidate shale typically requires a range of characteristics, including a relatively high total organic carbon (TOC) content, and it must be gas mature. Mechanical and dynamic elastic properties are also important shale characteristics that are not well understood as there have been a limited number of investigations of well-preserved samples. In this study, the elastic properties of shale samples are determined by measuring wave velocities. An array of ultrasonic transducers are used to measure five independent wave velocities, which are used to calculate the elastic properties of the shale. The results indicated that for the shale examined in this research, P- and S-wave velocities vary depending on the isotropic stress conditions with respect to the fabric and TOC content. It was shown that the isotropic stress significantly impacts velocity. In addition, S-wave anisotropy was significantly affected by increasing stress anisotropy. Stress orientation, with respect to fabric orientation, was found to be an important influence on the degree of anisotropy of the dynamic elastic properties in the shale. Furthermore, the relationship between acoustic impedance (AI) and TOC was established for all the samples.**

## KEYWORDS

Shale, anisotropy, ultrasonic waves, stress conditions, total organic content (TOC), lithology, acoustic impedance (AI).

## INTRODUCTION

Organic shale is a fine-grained sedimentary rock that is known to have a rich source of natural gas trapped inside it (Boyer et al, 2006). Candidate shales are typically required to have a high total organic content (TOC) to generate gas (Close et al, 2010). The elastic properties of shale rock vary significantly between, and in, reservoirs—due to variable material composition and fabric anisotropy exhibited by these organic-rich shales (Zhu et al, 2011). Organic shales are characterised by strong velocity anisotropy, low velocity and low density (Vernik and Nur 1992; Vernik and Liu 1997). Many shale-gas formations share properties, including low matrix porosity and low-permeability (Vernik et al, 2010). There is minimal understanding of their dynamic and elastic behaviour, however, due to a low volume of organic shale samples being described in literature, and the amount of time taken to test low-permeability samples (Dewhurst et al, 1998; Dewhurst et al, 2011). Indeed, many velocity measurements of shale have been conducted without controlling stress conditions, which is critical if the intent is to relate velocities to influences in effective stress conditions (Dewhurst and Siggins, 2006). Shale anisotropy has been recognised to be an issue with respect to depth conversion for seismic exploration, amplitude variation with offset (AVO), and imaging of structures in both seismic and crosshole tomography domains (Banik, 1984). Anisotropy can also be a source of significant errors in the estimation of the dynamic Poisson's ratio (Thomsen, 1986) and fluid identification (Sheriff, 2002). These shales exhibit significant mechanical anisotropy, due to the organised distribution of platy clay minerals (Zhu et al, 2011) and compliant organic materials (Vernik and Nur, 1992; Vernik and Liu, 1997; Sondergeld et al, 2000; Vernik and Milovac, 2011). There are also indications in literature that it is not only the amount of clay or organics influencing the anisotropy in organic rich shales, but also the maturity of the shales (Sone, 2012).

Few laboratory tests of the full elastic tensor and resultant anisotropy of shales, which take into account factors including porosity, smectite, kerogen content, and micro fractures, have been reported in literature (Vernik and Liu, 1997 ; Hornby, 1998). Recently, results of limited tests that included stress control, have shown that compaction fabrics, the orientation of stress anisotropy with deference fabric, and fracture orientation influence elastic properties (Delle Piane et al, 2011; Dewhurst et al, 2011); however, it is difficult to account for all the factors affecting the velocity and anisotropy of shale. In particular, factors including stress state, stress history, smectite content, and TOC content with pore fluid in situ are not widely reported (Bohacs et al, 2005; Passey et al, 2010). The controlling of laboratory experiments on well-characterised shales under in situ stress and stress conditions can help to study the impact of some of these factors on shale velocity and anisotropic response (Tutuncu, 2010). This research investigated the ultrasonic response of shale-gas samples from the Arrowsmith–2 well in the Perth Basin, with changing isotropic stress conditions. Specifically, the impact of TOC on shale-gas samples and the resultant impact on elastic wave velocities and their anisotropy was investigated.

### TOC content variations and AI

TOC is a major attribute of organic shale and is a measure of organic richness present in the shale The TOC content and thickness of the organic shale are key attributes that determine the economic viability of shale-gas (Ross and Bustin, 2009).

A good understanding of the effect of rock and pore fluid properties on seismic waves is important for the characterisation of a subsurface hydrocarbon reservoir based on seismic data (Sena et al, 2011). This information can be obtained using well logged data and laboratory experiments with samples cored from the well bore. Together with the seismic data, all of this information can be used to understand the entire dimension of the reservoir, providing valuable quantitative estimation of the TOC content and its impact (Zhu et al, 2011). Rock physics studies of organic shale have shown that the AI—the product of compressional velocity and density—decreases when the TOC is increased. Organic shale (TOC> 3%–4%) generally has significantly lower AI and higher intrinsic anisotropy than otherwise similar non-organic shale (Loseth et al, 2012). 'This gives the top and base of the source rock reflections characteristic negative and positive high amplitude, respectively, which dim with increasing reflection angle' (Loseth et al, 2012).

In this research, the TOC variations in the Carynginia and Kockatea shale formations in the Perth Basin were examined. Rock-Eval pyrolysis was used to identify the type and maturity of organic matter, and the amount of TOC content for a number of selected wells in the Perth Basin. Also, sonic velocity data and density data for the selected wells was provided by the Western Australia Department of Mines and Petroleum. Based on 45 samples, collected from the depths of 870 to 4,000 m, from 14 wells, the TOC present in the Kockatea shale varies from 0.2–1.3 wt% (Fig. 1A). Based on 30 samples from depth of 1,180 to 3,659 m from seven wells, the TOC present in the Carynginia ranges from 0.4 to about 4 wt% (Fig. 1B). There is a good correlation between TOC and AI for both the Kockatea shale and Carynginia Formations; as the TOC percentage increases the AI decreases. These correlations will be used to map variations in TOC profiles with local well calibration by converting seismic AI data to TOC content.

## METHODOLOGY

In this research, a mean effective stress, defined as $1/3\,(\sigma'1+2\sigma'3)$, was used as a standard triaxial test. An in-depth discussion of this test has been written by Dewhurst and Siggins (2006). Hooke's law describes the mechanical behaviour of a linear elastic body; the law states that for such a body, stress and strain can be related through a fourth–order tensor *Cijkl* (Mavko et al, 1998). For an anisotropy elastic rock exhibiting vertical transverse, isotropy (VTI) is given in a Cartesian coordinate, shown in Equation 1.

$$\begin{bmatrix} \sigma_{xx} \\ \sigma_{yy} \\ \sigma_{zz} \\ \sigma_{yz} \\ \sigma_{xz} \\ \sigma_{xy} \end{bmatrix} = \begin{bmatrix} C_{11} & C_{12} & C_{13} & 0 & 0 & 0 \\ 0 & C_{11} & C_{13} & 0 & 0 & 0 \\ 0 & 0 & C_{33} & 0 & 0 & 0 \\ 0 & 0 & 0 & C_{44} & 0 & 0 \\ 0 & 0 & 0 & 0 & C_{44} & 0 \\ 0 & 0 & 0 & 0 & 0 & C_{66} \end{bmatrix} \begin{bmatrix} \varepsilon_{xx} \\ \varepsilon_{yy} \\ \varepsilon_{zz} \\ \varepsilon_{yz} \\ \varepsilon_{xz} \\ \varepsilon_{xy} \end{bmatrix} \quad (1)$$

From the matrix, Z lies along the symmetry axis, the elastic stiffness coefficients (*Cij*), $\sigma xx,yy,zz$ are normal stresses, σzx,yz,xy are shear stresses,$\varepsilon xx,yy,zz$ are normal strains, and εzx,yz,xy are shear strains are shear strains. Velocities and elastic constants are related and the equations can be found in Dewhurst and Siggins, 2006. In this research, the isotropic stress state was applied equally in all directions, the shale was cut parallel to the bedding as it was presumed to be transversely isotopic (TI), and all the three principal stresses were presumed to be equal.

Due to the fine-grained nature of shales and their challenging characteristics, it is important to use special techniques to ensure samples are tested in as close to a representative state as possible (Prasad et al, 2009). This is important to avoid the desiccation of shales after coring, which would cause the shale to fracture, inducing large capillary stresses and changing the particle orientation and pore size distribution (Tutunce, 2010; Dewhurst et al, 2011). The shale samples used in this research are from the Arrowsmith–2 well, taken at three different depth intervals and three TOCs (0.23%, 1.8% and 3.03%). The samples were cylindrical (about 76 mm in length and around 38 mm in diameter), and offcuts from those samples were used for sample characterisation to measure grain size distribution, pore size distribution, porosity, composition and grain density. It was necessary to obtain proprietary information before testing the samples, and this information included the depth, age and TOC content of the samples. The main issues in measuring elastic properties of shale and clay minerals are due to their small grain size, and low-permeability (Horsrud et al, 1998; Prasad et al, 2009).

### Ultrasonic measurements

In this research, new equipment that allows an understanding of the physical properties of shale under well-constrained laboratory conditions was used. This equipment contains a high pressure and temperature triaxial cell, simulating natural in situ conditions and examining the changes in the physical properties of the rock. The rig provides independent control of the mean effective stress to operational upper limits of 35 MPa for all the three principal stresses on specimens of 38 mm diameter. All of the tests were measured at normal room temperature; data logging and pump control were based on a LabVIEW program. Additional details on this equipment can be found in Dewhurst and Siggins (2006) and Delle Piane et al (2011).

'The velocities measured tests are: (Vpv) is the P-wave that travel normal to bedding plane (Vph) is the P-wave propagate parallel to bedding, (qVp45) is the quasi-P-wave propagating at 45° to bedding, (Vsv) is the wave propagate normal to bedding with particle motion parallel to bedding, (Vsh) S-wave that travel parallel to bedding with particle motion parallel to bedding', (Delle Piane et al, 2011).

An experimental configuration (Fig. 2), the same as that described by Dewhurst and Siggins (2006), was used in this research. This permits the full elastic tenser to be calculated from a single core, assuming the shale is a TI medium. Five independent elastic coefficients are required for the full description of its elastic response, and the symmetry plane of such coincides with the fabric/bedding plane. The end platens house one MHz, PZT-5H piezo-ceramic P- wave and S-wave element, that measures the wave velocities down the core axis. Furthermore, radial P-wave and S-wave transducers are attached to the membrane to measure the velocity crossing the core diameter. Also, a couple of P-wave elements—directly attached to the sample surface—transmit and receive pulses at 45° to the core axis (Delle Piane et al, 2011). This configuration was necessary in order to make all measurements for the determination of the stiffness tensor on a single core and calculate anisotropy, with the shale principal axes aligned with the cell rather than using a few core plugs cut at different angles to the principal axes (Hornby, 1998; Sondegeld and Chandre 2011). Five independent wave velocities are measured with the ultrasonic transducer array, presented in Figure 3.

### Shale composition and microstructure

The composition of the whole rock mineralogy for the Arrowsmith–2 well in the Perth Basin is shown in Table 1. Quartz is abundant in the four samples (comprising of 25%–54%, by weight). Plagioclase is the second most abundant mineral in

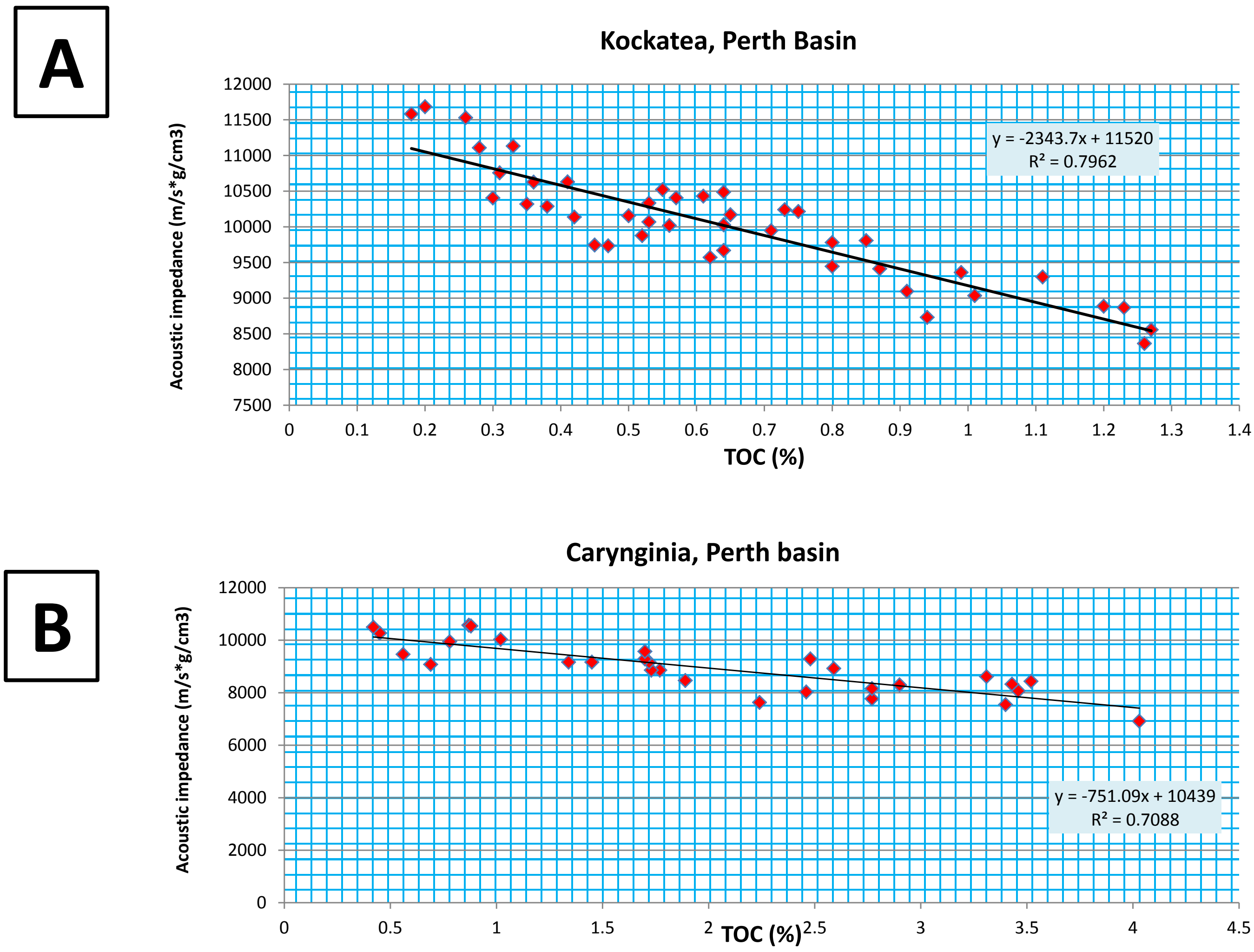


**Figure 1.** The relationship between the TOC percent (measured by Rock-Eval pyrolysis from samples cored) and AI (from sonic log and density log) in the Kockatea (A) and Caryngina (B) shale formations in different wells in the Perth Basin.

the four samples (comprising of 6%–11%, by weight). Feldspar has the same abundance in all samples (comprising of about 4%, by weight).

Quantitative whole rock analysis results showed that the clay minerals collectively made up between 56% and 28% of the samples. Illite/mica had the highest content of clay minerals in the four samples, which comprised 25% to 16%, by weight. The second highest content of clay minerals was illite/semectite with 10%–20%, by weight. Other clay minerals that were abundant in the four samples comprised of slightly below 7%, by weight. From these results, it is clear that the total clay minerals content percentage was raised when the TOC content was increased and the quartz content decreased. This finding requires further study and more samples will need to be taken and analysed to find the relationships between TOC content and clay minerals and between TOC content and non-clay minerals respectively.

The physical properties of the Arrowsmith–2 well are shown in Table 2. All of the shale samples have similar ranges of bulk density, ranging from 2.619 ($^g/_{cc}$) to 2.648 ($^g/_{cc}$). The grain density ranged from 2.630($^g/_{cc}$) to 2.674($^g/_{cc}$). The effective porosity percentages for all the samples were 2.6%, 3.01%, 3.23% and 2.93%. The shale samples used in this research were selected based on the TOC content, enabling a study of the impact of TOC on the physical properties and ultrasonic velocities. The highest percentage of TOC was 3.03%, by weight (found in A.C.01), and the lowest percentage was about 0.23%, by weight (found in A.C.10).

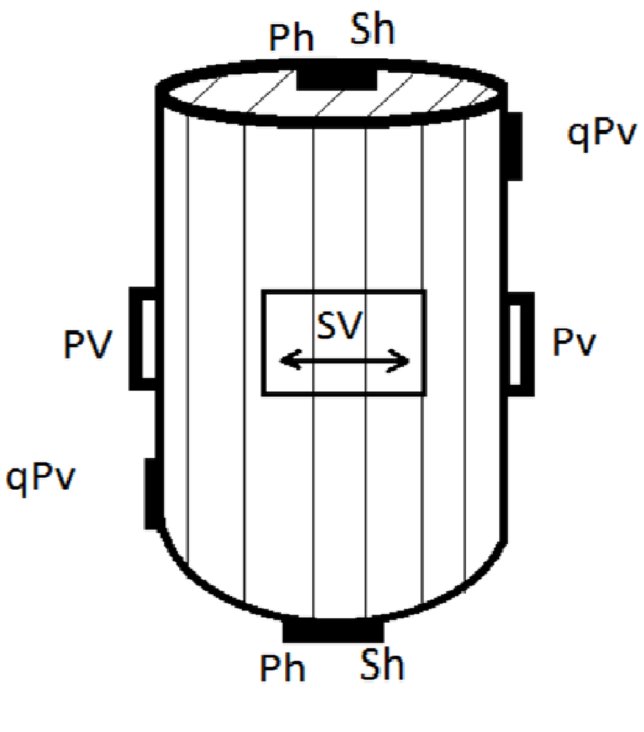


**Figure 2.** The configuration of the triaxial rig, showing the isotropic stress (applied equally in all directions) and the location of ultrasonic transducers with respect to the bedding.

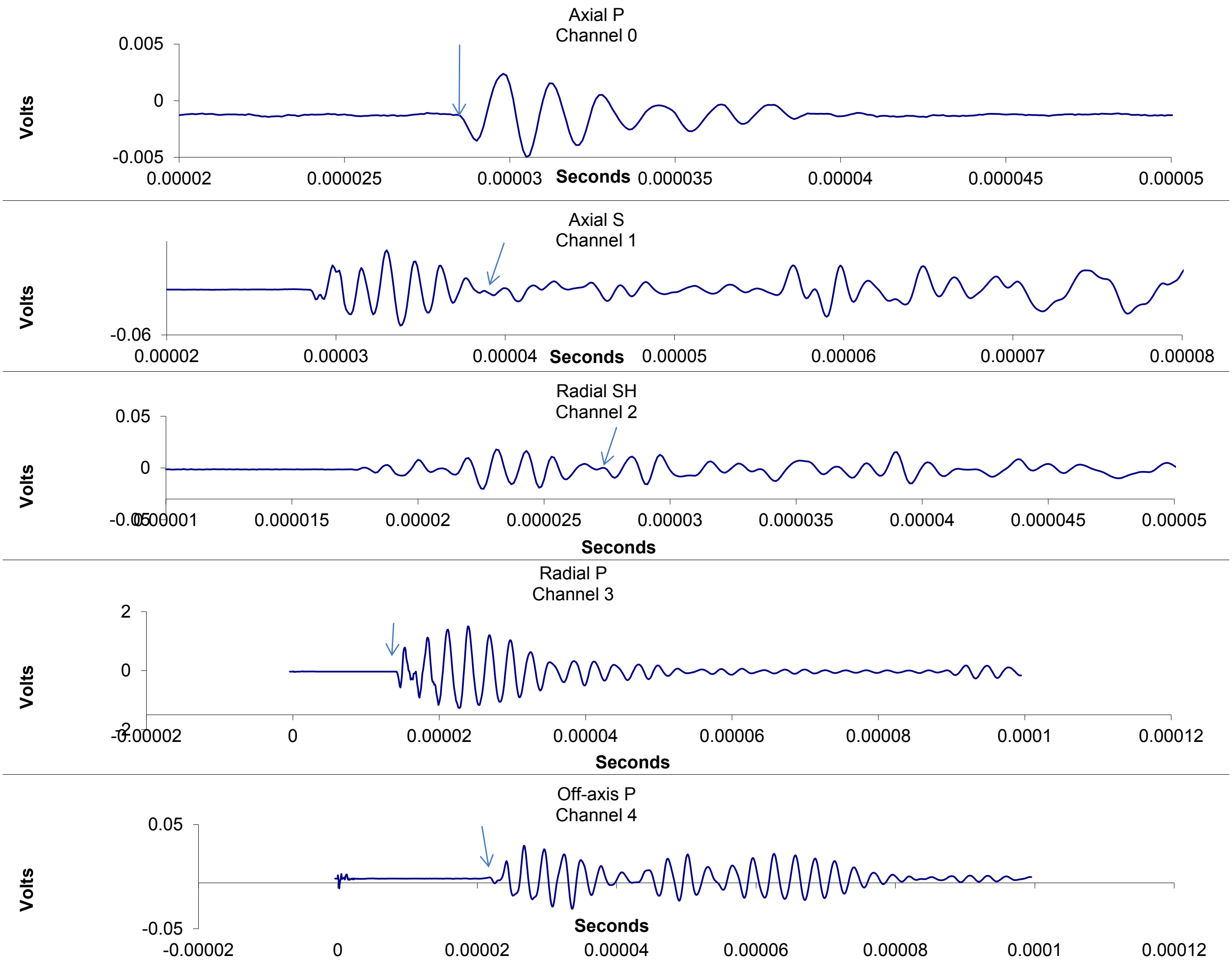


**Figure 3**. Examples of waveforms from the tests on the Arrowsimth-2 shale; axial P-and S waves are *Vph* and *Vsh* and radial P- and –S waves are *Vpv* and *Vs1*. The off axis P-wave is at 45° to the bedding. These velocities measured at nominal centre frequencies of 0.6-1.0 MHz for P-waves to 0.2-0.4 MHZ for s waves.

**Table 1.** X-Ray diffraction data—whole rock and clay mineralogy for different shale samples from the Arrowsmish–2 well.

| SAMPLE ID | DEPTH (m) | QUARTZ | K-FELDSPAR | PLAGIO-CLASE | CALCITE | SIDERITE | ANKERITE/ FE-DOL | DOLOMITE | PYRITE | BARITE | MAGNE-TITE | TOTAL NON-CLAY | SMECTITE | ILLITE/ SMECTITE (I/S) | ILLITE+ MICA | KAOLINITE | CHLORITE | TOTAL CLAY | GRAND TOTAL |
|---|---|---|---|---|---|---|---|---|---|---|---|---|---|---|---|---|---|---|---|
| A.C.1 | 2,780.3 | 25 | 4 | 6 | 4 | 1 | 0 | 0 | 4 | 0 | 1 | 44 | 2 | 20 | 25 | 3 | 7 | 56 | 100 |
| A.C.8 | 2,806.2 | 41 | 4 | 8 | 1 | 2 | 1 | 0 | 3 | 1 | 0 | 59 | 1 | 15 | 19 | 1 | 5 | 41 | 100 |
| A.C.9 | 2,812.6 | 54 | 4 | 8 | 1 | 1 | 2 | 0 | 2 | 0 | 0 | 72 | 2 | 10 | 12 | 1 | 3 | 28 | 100 |
| A.C.10 | 2831.1 | 45 | 4 | 11 | 2 | 2 | 1 | 1 | 1 | 1 | 0 | 67 | 2 | 10 | 16 | 1 | 4 | 33 | 100 |

**Table 2.** Physical properties for the Arrowsmish–2 well for different shale samples.

| Sample ID | Depth (m) | As Received Bulk Density (g/cc) | As Received Grain Density (g/cc) | Effective Porosity (%) | TOC (WT%) |
|---|---|---|---|---|---|
| A.C.1 | 2,780.32 | 2.619 | 2.63 | 2.67 | 3.03 |
| A.C.8 | 2806 | 2.619 | 2.632 | 3.01 | 1.8 |
| A.C.9 | 2,812.62 | 2.615 | 2.653 | 3.23 | 1.08 |
| A.C.10 | 2,831.15 | 2.648 | 2.674 | 2.93 | 0.23 |

## RESULTS

The aim of this research was to examine the elastic wave velocities and their anisotropy with varying stress levels. The impact of the mean effective stress on the ultrasonic velocity in the Arrowsmith–2 shale samples is presented in Figure 4(A). The first test of shale was sampled using a horizontal core plug from A.C.08, and showed a TOC content of 1.8%, by weight; the velocity of *Vph* increased from 4,171m/s to 4,575 m/s as the mean effective stress increased from 0.7 MPa to 38 MPa. The velocity of *Vpv* increased from 3,290–4,293 m/s over the same stress range. The quasi-P velocity increased from 3,707m/s to 4,392 m/s over the range of 0.7MPa–38 MPa and was, therefore, between the range of *Vph* and *Vpv*. The *VSh* increased from 2,500 m/s to 2624 m/s, while *Vsv* increased from 2,229 m/s to 2346 m/s as the mean effective stress increased from 0.7MPa–38 MPa. The *Vph/Vsh* ratio increased slightly from 1.7 to 1.77 by increasing the mean effective stress within the same stress range, shown in Figure 5(A). The *Vpv/Vsv* ratio also increased from 1.5 to 1.85 over the same stress range.

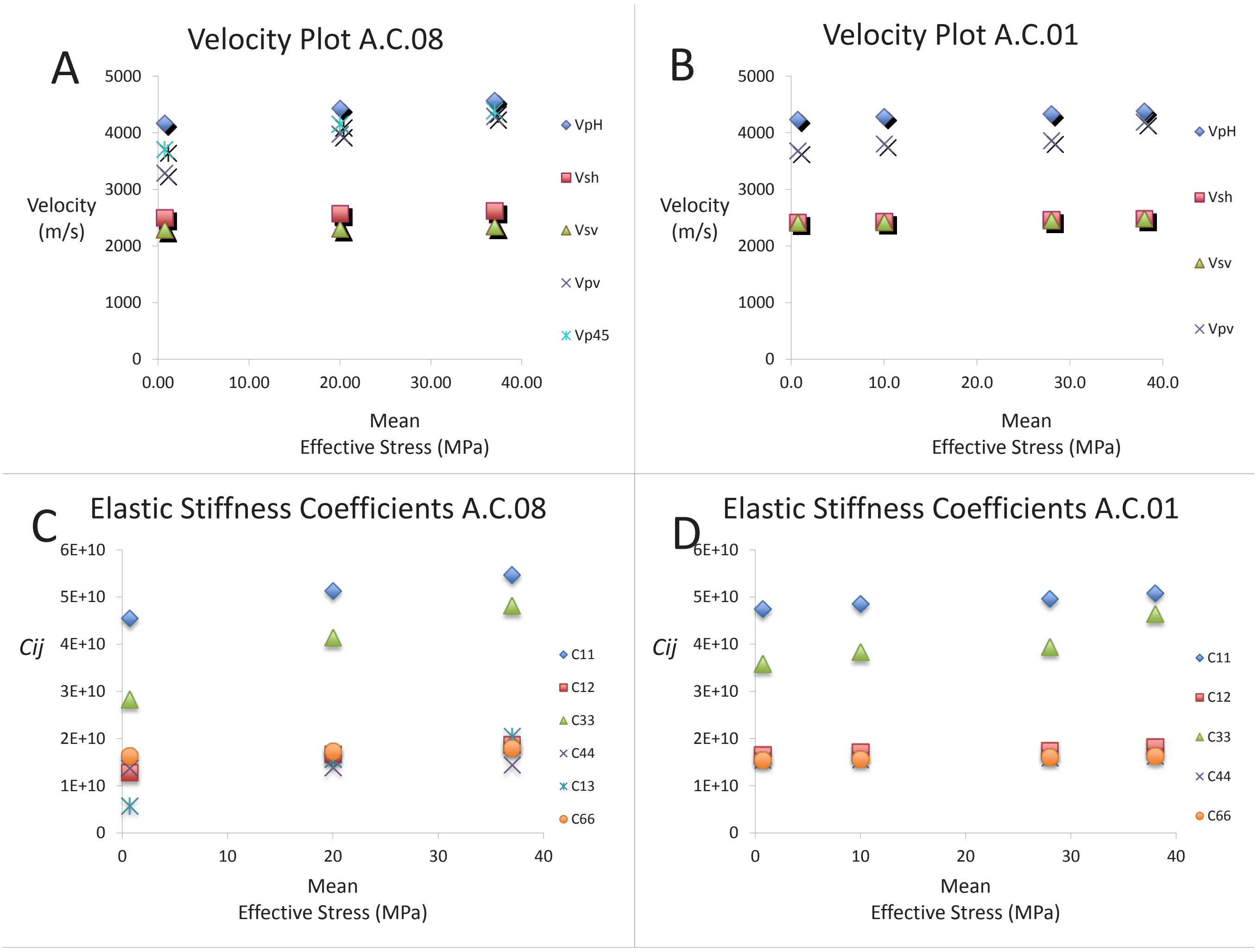


**Figure 4.** The relationship between velocities and mean effective stress for the Arrowsmish-2 well samples A.C.08 (A) and A.C.01 (B), the velocities increase as the mean effective stress increases. The responses of elastic constants to increase the mean effective stress for Arrowsmish-2 well shale sample A.C.08 (C) and sample A.C.01 (D).

The second test of shale was sampled using a vertical cut core plug from A.C.01, and showed a TOC of 3.03%, reported in Figure 4(B). The velocity of *Vph* increased from 4,237 m/s to 4,385 m/s as the mean effective stress increased from 0.7 MPa to 38 MPa, while *Vpv* increased from 3,682 m/s to 4,191 m/s over the same stress range. The *VSh* increased from 2,420 m/s to 2,484 m/s, while *VSv* increased from 2,414 m/s to 2,483 m/s as the mean effective stress increased from 0.7 MPa to 38 MPa. Unfortunately, the electrical connection for the quasi-P velocity was lost early in the experimental cycle and, therefore, these waveforms were not recorded. Figure 5(B) shows the *Vph/Vsh* ratio also increased from 1.7 to 1.78 over the same stress range. The *Vpv/VSv* ratio increased slightly from 1.52 to 1.8 when the mean effective stress increased in the range of 0.7–38 MPa.

The third shale sample test, A.C.10 (a horizontal cut), in Figure 6(A) showed a TOC of 0.23%. The velocity of *Vph* increased from 4,502.6 m/s to 4,909 m/s as the mean effective stress increased from 0.7 to 38 MPa. The *Vpv* increased from 4,259.5 m/s to 4,293 m/s over the same stress range. The quasi-P velocity increased from 4,283.5 m/s to 4,443.7 m/s over the same stress range and was, therefore, between *Vph* and *Vpv.* The *Vsh* increased from 2,905 m/s to 3,208 m/s, while *VSv* increased from 2,639 m/s to 4,293 m/s as the mean effective stress increased from 0.7–38 MPa. These results suggest that the velocity increased and the errors decreased with rising stress levels. The errors in the S-wave velocity were approximately 7% at lower stress levels. P-wave errors were small at all stress levels used in this research. In addition, the shales used in this research showed a high degree of anisotropy in velocity.

The responses of the elastic coefficients of the samples from A.C.08 (*C11, C33, C44, C66, C12* and *C13*) are shown in Figure 4(C). The *C1* increased from 45.5 GPa to 54.7 GPa, while *C33* increased from 28.3 GPa to 48.2 GPa as the mean effective stress increased from 0.7 MPa to 38 MPa. Both *C44* and *C66* increased over the same stress range from 13.7 GPa to 14.1 GPa and 16.4 GPa to 17.9 GPa, respectively. *C12* increased from 12.8 GPa to 18.8 GPa, *C13* increased from 5.7 GPa to 20.4 GPa as the mean effective stress increased from 0.7 MPa to 38 MPa. The second test of shale sample from A.C.01 in Figure 4(D), showed that the *C11* increased from 47.5 GPa to 50.9 GPa, while *C33* increased from 35.8 GPa to 46.4 GPa as the mean effective stress increased from 0.7 MPa to 38 MPa. Both *C44* and *C66* increased from 15.4 GPa to 16.3 GPa and 15.4 GPa to ~16.3 GPa over the same stress range respectively. *C12* increased from 16.3 GPa to 18.2 GPa.

The elastic coefficients calculated were used from Thomsen parameters to derive the an-isotropy parameters (Thomsen, 1986). The impacts of mean effective stress on P-wave ($\varepsilon$) and S-wave ($\gamma$) anisotropy factors, as well as the wave front anellipticity factor ($\delta$), are shown in Figure 7 (A) for sample A.C08. Initial anisotropy at low stress is seen to be large (0.30 for P waves, 0.10 for S-waves) and variable with changing mean effective stress, and $\varepsilon$ decreased from 0.3 to 0.07 as the mean effective stress increased from 0.7 MPa to 38 MPa. Initially, $\gamma$ was stable around 0.13 as the stress increased,

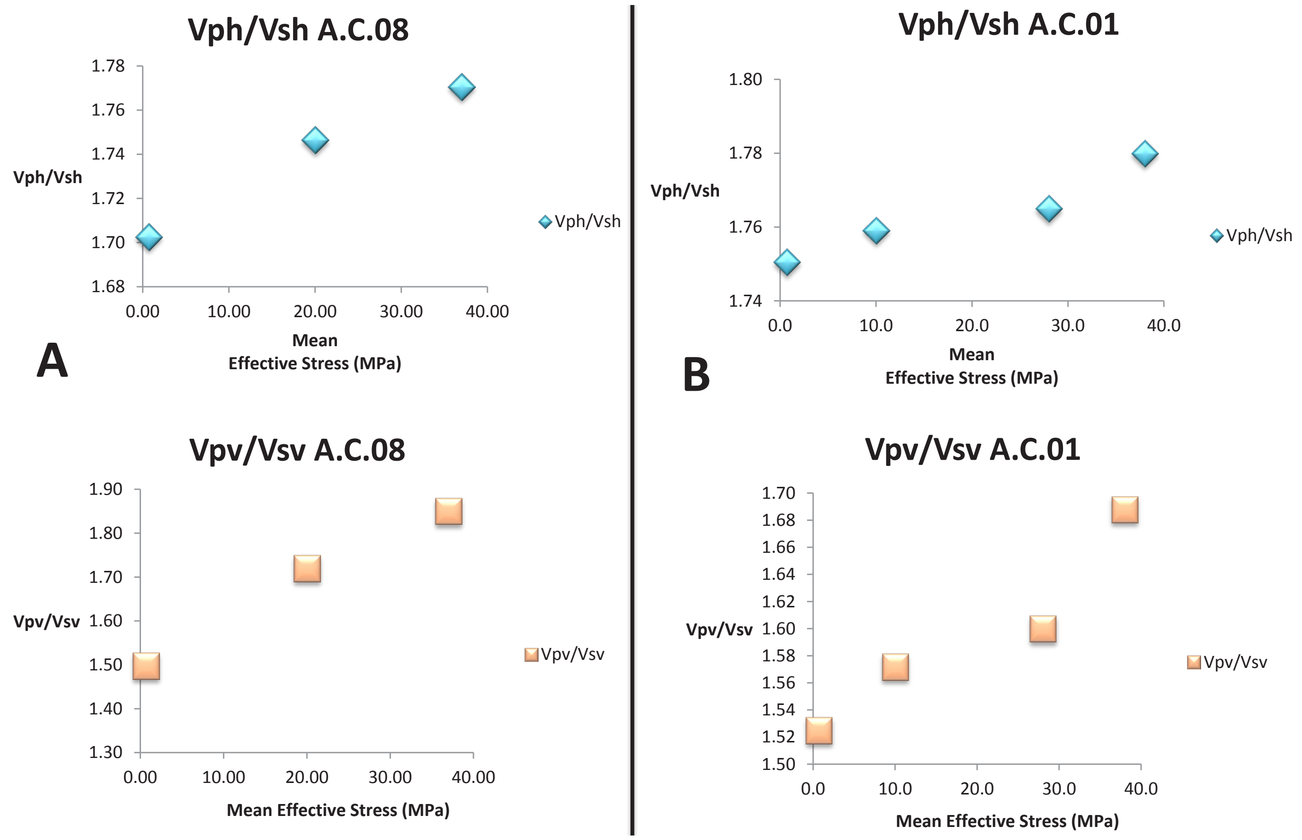


**Figure 5**. The influence of the mean effective stress on Vp/Vs ratios in the Arrowsmish-2 well shale.

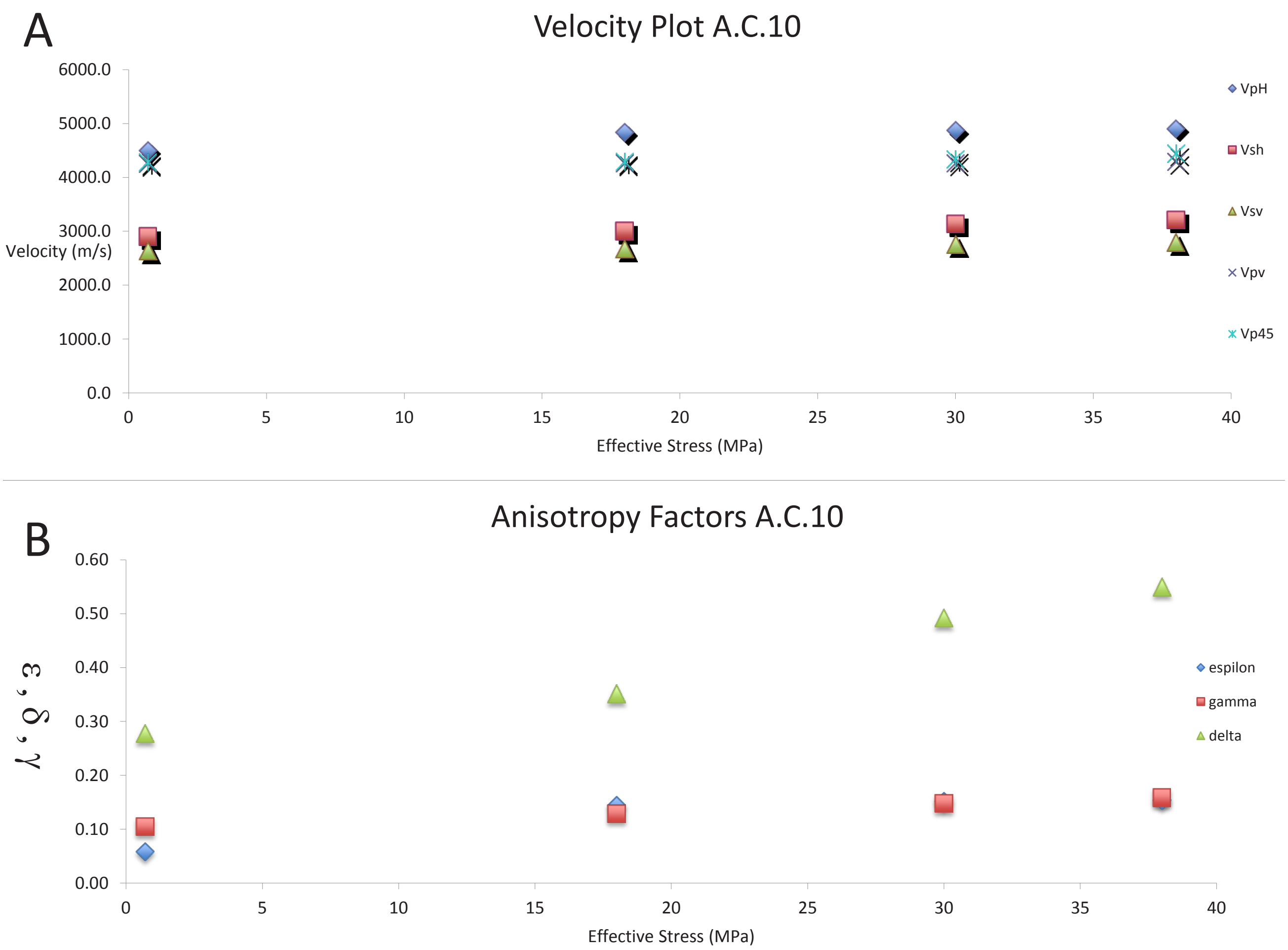


**Figure 6**. The relationship between velocities and mean effective stress for Arrowsmish–2 well shale sample ID A.C.10. (A) the velocities increase with the mean effective stress. (B) The influence of mean effective stress on ε, γ and δ for Arrowsmith–2 well shale sample A.C.10.


**Figure 7.** Influence of mean effective stress on ε, γ and δ for Arrowsmith–2 well shale sample A.C.08 (A) and A.C.01(B).

however δ dropped from 0.19 to 0.02 as mean effective stress increased from 0.7MPa to 38 MPa. Results of the second test of the shale sample from A.C.01, in Figure 7 (B), showed that at low stress the initial anisotropy was lower than the first sample and variables with changing mean effective stress. As the mean effective stress increased from 0.7 MPa to 38 MPa, ε decreased from 0.16 to 0.05. Initially, γ was stable at around 0.01 as the stress increased. Errors in elastic constants were <1%—with the exception of *C13*, where errors were approximately 2%—while errors in the anisotropy parameters were higher due to the use of ratios of elastic constants. Using these ratios, errors in ε and γ can be up to 2%, while δ has the least accuracy, with errors of typically±13% (Dewhurst and Siggins, 2006).

Three shale core plug samples were tested from the Arrowsmith–2 well, which were moderately anisotropic and loaded parallel to bedding. The anisotropy parameters were sensitive to changes in confining pressures. Velocity anisotropy (A), as described in (Dewhurst et al, 2011), is shown in Figure 6(B) and 7(A and B); ε (epsilon) in sample A.C.08 decreased as the confining pressure increased. This was also reported in the samples A.C.01. Over the entire range of stress levels in the samples A.C.08 and A.C.01 sites, however, γ (gamma) was stable. In the third shale sample A.C.10, ε and γ were stable over the entire range of stress levels.

## DISCUSSION

Three samples of shale-gas from the Arrowsmith–2 well were ultrasonically tested in a changing stress field simulation of an undrained tectonic deformation. The key controls on the elastic properties of organic shale were effective stress, TOC content, porosity and clay content. High TOC shales are generally characterised by strong velocity anisotropy and low velocity in the beddings normal direction, and relatively low density and porosity (e.g., Vernik and Nur, 1992; Vernik and Liu, 1997; Sondergeld et al, 2000). The intrinsic anisotropy increased with rising TOC (Tutuncu, 2010). Therefore, the velocities of organic-rich shales decreased with rising TOC. Figure 8 (A) shows the relationships between different TOCs (0.23, 1.8 and 3.03%) and the velocities of shale samples. In this research, we have selected the velocities at 38 MPa in situ effective stress values as the reservoir condition. It was clear from the results that all of the velocities decreased with rising TOC. The *Vph* of three samples (A.C.10, A.C.08 and A.C01) decreased from 4,908.9 m/s to 4,385.3 m/s as the TOC percentage increased. Furthermore, *VSh* decreased from 3,208.3 m/s to 2,484.3 m/s over all the three samples, while the TOC percentage increased. The last two waves, *VSh* and *VSh,* increased as the TOC percent rose. Loseth et al (2012) studied the relationships between the TOC of organic rich claystones and AI, which is the product of compressional velocity and density. The studies showed that AI decreases nonlinearly with increasing TOC.

The key finding from this research is that the velocities in the shale samples—P and S waves and Cij—responded in similar ways with changes in the mean effective stress levels. The shale samples were found to have a high degree of innate anisotropy resulting from their fine grain size, strong compaction fabric, composition and the presence of stress relief microfractures in the cores. The results show that the velocities increased with the mean effective stress across the whole stress range. This was also found in previous work on ultrasonic characterisation on shale under the same conditions (e.g., Dewhurst and Siggins, 2006; Dodds et al, 2007; Delle Piane et al, 2011; Dewhurst et al, 2011). Changes in ultrasonic anisotropy occurred mainly as a result of changes in the magnitude of the mean effective stress, as well as the orientation and degree of anisotropy of the stress field. Increasing in the mean effective

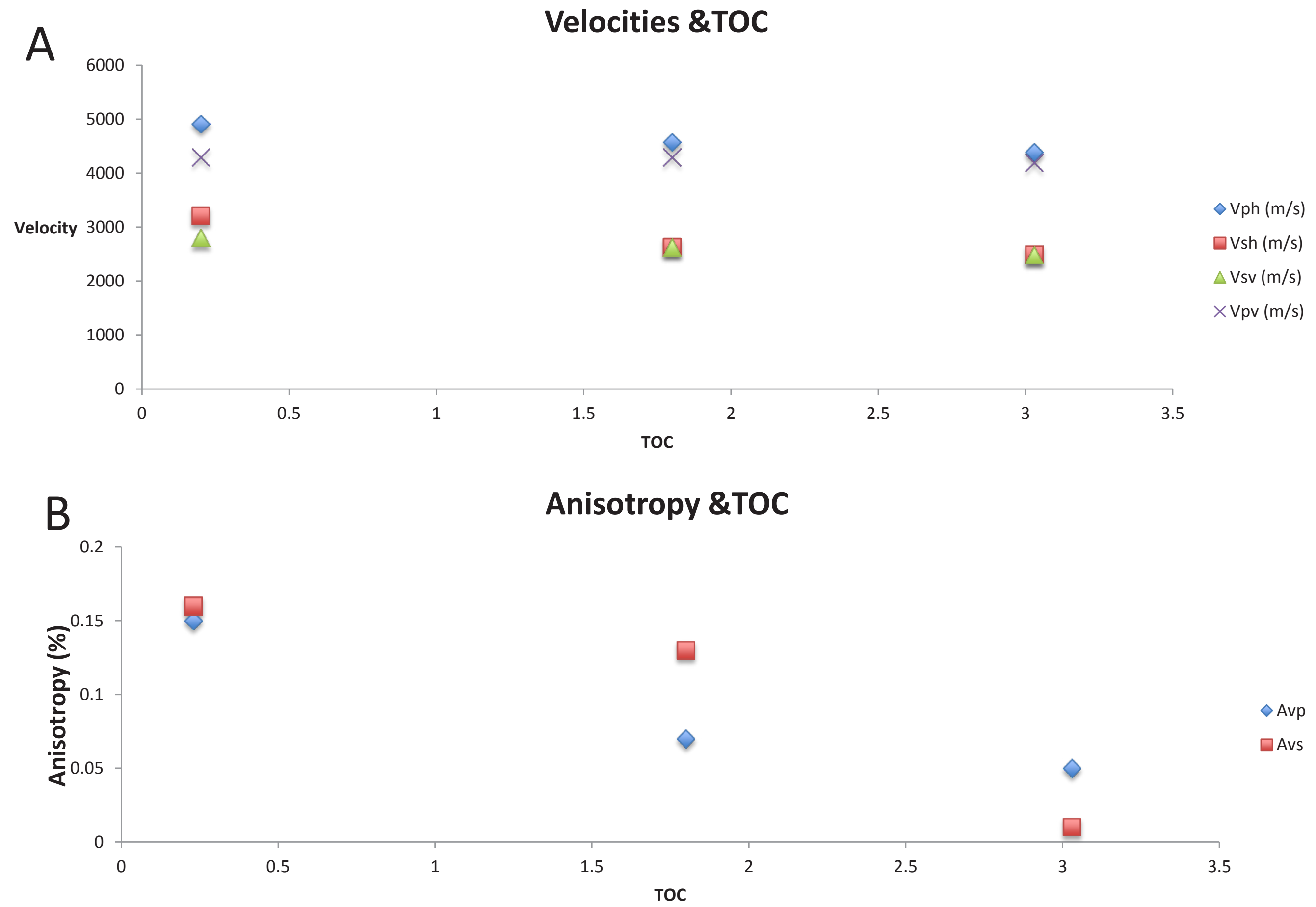


**Figure 8.** (A) the impact on the velocities from different percentages of TOC in the Arrowsmish-2 well. (B)the impact on the Anisotropy velocities between different percentages of TOC in the Arrowsmish-2 well.

stress decreased the ultrasonic anisotropy, but this decrease was shown to be dependent on the degree of stress anisotropy (Figure 8, B). Tutuncu (2010) found that an:

> 'anisotropy drop with increasing mean effective stress at low stresses implying the high degree of anisotropy is closely associated with present of fractures. The increase of the stress results in the closure of most of the factures reducing the degree of the anisotropy.'

Dewhurst et al (2011) noted the ultrasonic anisotropy decreases in a changing isotropy stress field, rather than a changing the anisotropic stress field. The results showed that there was stress sensitivity and researchers should be careful when using isotopic approaches when dealing with compacted rich shales due to their highly anisotropic nature and likely compositional effects on velocity.

In addition, the results of this research show that as the clay mineral content increases in the shale, the velocity will decrease. X-Ray diffraction data from this research showed that the clay mineral content increased from 33% to 56% by weight and the velocities decreased. Furthermore, high TOC shale is characterised by low density and low porosity. From the physical properties table (Table 2), it is clear that the density and the porosity decreased as the TOC percentage increased over all of the core plug shale samples (A.C.10, A.C.08 and A.C.01).

## CONCLUSIONS

The results of this research showed the main controls on the elastic properties of organic rich shales, and investigated the impact of TOC content and the stress field on elastic wave velocities and their anisotropy. Ultrasonic velocity was measured in a changing stress field simulated under tectonic deformation using three shale core samples from the Arrowsmish-2 well in the Perth Basin. Laboratory measurement was used to estimate the elastic anisotropy, as it is a key to defining symmetries and the magnitude of anisotropy. It also indicates that weak anisotropy can be revealed by measuring wave velocities using a new method. An array of ultrasonic transducers was used to measure five independent wave velocities. To study the influence of the TOC percentage, samples were selected in different TOCs (0.23%, 1.8% and 3.03%). The results showed evidence of stress sensitivity and that there were challenges when dealing with compacted rich shales due to their highly anisotropic nature and likely compositional effects on velocity. The velocities increased with the stress levels, signifying a progressive rise in the stiffness of the sediment associated with the crack closure. Also, the results of the research showed that the velocities decreased as the TOC percentage increased. In addition, other factors including porosity, concentration of clay minerals and density have an influence on the elastic waves of organic shale.

## ACKNOWLEDGEMENTS

The authors would like to thank Curtin University's Shale-gas Consortium sponsors; the Western Australian Department of Mines and Petroleum, Buru Energy, Carnarvon Petroleum, Norwest Energy and Woodside for financial support and permission to publish the results of this study. The authors would also like to thank Norwest Energy for providing the shale samples, TOC data and X-Ray data from the Arrosmith–2 well.

## REFERENCES

BANIK, N.C., 1984—Velocity anisotropy of shales and depth estimation in the North Sea basin. In: Geophysics, 49 (9), 141–1,419.

BOHACS, K.M., GRABOWSHI, G.J., CARROLL,A. R.,MANKIEWICZ, P.J., MISKELL-GRAHARDT, K.J., SCHWALBACH, J.R., WEGNER, M.B., AND SIMO, J.A., 2005—Production,destruction, and dilution—the many paths to source-rock development. In: The Deposition of Organic-Carbon-Rich Sediments: Models, Mechanisms, and Consequences, SEPM Special Publications, 82, 61–102.

BOYER, C., KIESCHNICK, J., SUAREZ-RIVERA, R., LEWIS, R.E., AND WATERS, G., 2006—Producing gas from its source. In: Oilfield Review, Autumn, 36-49.

CLOSE, D., STIRLING S., CHO, D.,HORN, F., 2010—An integrated workflow for shale-gas in the Western Canadian sedimentary basin: Surface seismic to stimulation. AAPG 2010 Annual Convention, New Orleans, Louisiana, 11–14 April, 40569.

DODDS, K.J., DEWHURST, D.N., SIGGINS, A.F., CIZ, R., UROSEVIC, M., GUREVICH, B., AND SHERLOCK, D.H., 2007—Experimental and theoretical rock physics research with application to reservoirs, seals and fluid processes. In: Journal of Petroleum Science and Engineering, 57, 16–36.

DELLE PIANE, C., DEWHURST, D., SIGGINS, A., AND RAVEN, M., 2011—Stress-induced anisotropy in brine saturated shale. In: Geophysical Journal International, 184 (2), 897–906.

DEWHURST, D.N., SIGGINS, A.F., SAROUT, J., RAVEN, M. D., NORDGÅRD-BOLÅS, H.M., 2011—Geomechanical ultrasonic characterization of a Norwegian sea shale. In: Geophysics, 76 (3), Special section—seismic anisotropy.

DEWHURST, D.N., SIGGINS, A.F., 2006—Impact of fabric, microcracks and stress field on shale anisotropy. In: Geophysical Journal International, 165 (1), 135–148.

DEWHURST, D.N., APLIN, A. C., SARDA, J. P., AND YANG. Y., 1998—Compaction-driven evolution for porosity and permeability in natural mudstones: An experimental study. In: Journal of Geophysical Research: Solid Earth 103 (B1), 651–661.

HORSRUD, P., SØNSTEBØ E. F., AND BØE, R.,1998—Mechanical and petrophysical properties of North Sea shales. In: International Journal of Rock Mechanics and Mining Sciences, 35 (8), 1,009–1,020.

HORNBY, B.E., 1998—Experimental laboratory determination of the dynamic elastic properties of wet, drained shales. In: Journal of Geophysical Research: Solid Earth, 103 (B12), 29,945–29,964.

LØSETH, H., WENSAAS, L., GADING, M., DUFFAUT, K., AND SPRINGER, M., 2012—Can hydrocarbon source rocks be identified on seismic data? In: Geology, 39 (12), 1,167–1170 .

MAVKO, G., MUKERJI, T., AND DVORKIN, J., 1998—The rock physics handbook: Tools for seismic analysis in porous media. Cambridge: Cambridge University Press.

PASSEY, Q.R., BOHACS, K.M., ESCH, W.L., KLIMENTIDIS, R., AND SINHA, S., 2010— From oil-prone source rock to gas-producing shale reservoir - Geologic and petrophysical characterization of unconventional shale gas reservoirs. International Oil and Gas Conference and Exhibition, Beijing, China, 8-10 June, 131350-MS.

PRASAD, M., PAL-BATHIJA, A., JOHNSTON, M., RYDZY, M., AND BATZLE, M., 2009—Rock physics of the unconventional. In : The Leading Edge, 28 (1), 34–38. doi:10.1190/1.3064144.

ROSS, D.J.K., AND BUSTIN, R. M., 2009—The importance of shale composition and pore structure upon gas storage potential of shale-gas reservoirs. In: Marine and Petroleum Geology, 26, 916–927.

SENA, A., CASTILLO, G., CHESSER, K., VOISEY, S., ESTRADA, J., CARCUZ, J., CARMONA, E., AND HODGKINS, P., 2011—Seismic reservoir characterization in resource shale plays: Stress analysis and sweet spot discrimination. In: The Leading Edge, 30, 758–764.

SHERIFF, R.E., 2002—Encyclopedic dictionary of applied geophysics. In: Geophysical Reference Series, 13, SEG, 429 pp.

SONE, H., 2012—Mechanical properties of shale-gas reservoir rocks and its relation to the in situ stress variation observed in shale-gas reservoirs. In: Stanford University, SRB volume 128.

SONDERGELD, C.H., RAI, C.S., MARGESSON, R.W., AND WHIDDEN, K.J., 2000—Ultrasonic measurements of anisotropy on Kimmeridge shale. 70th Annual International Meeting, SEG, Expanded Abstracts, 1,858–1,861.

THOMSEN, L., 1986—Weak elastic anisotropy. In: Geophysics, 51 (10), 1,954–1,966.

TUTUNCU, A.N., 2010—Anistropy, compaction and dispersion characteristics of reservoir and seal shales. 44th U.S. Rock Mechanics Symposium and 5th U.S.-Canada Rock Mechanics Symposium, June 27–30, Salt Lake City, Utah, 10–344.

VERNIK, L., AND KACHANOV, M., 2010—Modeling elastic properties of siliciclastic rocks. In: Geophysics, 75 (6), 171–182.

VERNIK, L., AND LIU, X., 1997—Velocity anisotropy in shales: A petrophysical study. In: Geophysics, 62 (2), 521–532.

VERNIK, L., AND MILOVAC, J., 2011—Rock physics of organic shales. In: The Leading Edge, 30 (3), 318–323.

VERNIK, L., AND NUR, A., 1992—Ultrasonic velocity and anisotropy of hydrocarbon source rocks. In: Geophysics, 57 (5), 727–735.

ZHU, Y., LIU, E., MARTINEZ, A., PAYNE, M.A., HARRIS, C.E, 2011—Understanding geophysical responses of shale-gas plays. In: The Leading Edge, 30 (3), 332–338.

*Authors' biographies next page.*

## THE AUTHORS

**Yazeed Altowairqi** is a PhD student in the Department of Petroleum Engineering at Curtin University. His research focuses on rock physics of high TOC shale-gas and the seismic response of shale. His study examines various applications of seismic inversion and mulit-attribute analysis though acoustic and shears impedance analysis. Yazeed is also trying to build a rock physics model of shale-gas formations from well log data and calibrating it to laboratory results. Yazeed was awarded his Masters degree in geophysics in 2010 from Curtin University after completing his BSc, also in geophysics, in 2007 from King Abdulaziz University (KAAU).

*y.altowairqi@postgrad.curtin.edu.au*

**Assoc. Professor Reza Rezaee**, of Curtin University's Department of Petroleum Engineering, has a PhD in reservoir characterisation. He has more than 25 years' experience in academia; during his career he has been engaged in several research projects supported by national and international oil and gas companies, and these commissions, together with his supervisory work at various universities, have involved a wide range of achievements. Reza has supervised more than 60 MSc and PhD students during his university career to date. He has published more than 120 peer-reviewed journal and conference papers, and is the author of three books on petroleum geology, logging, and log interpretation. Reza's research has been focused on integrated solutions for reservoir characterisation, formation evaluation, and petrophysics. He has utilized expert systems, such as artificial neural networks and fuzzy logic, and has introduced several new approaches to estimate rock properties from log data, where conventional methods have failed to succeed. Presently, he is focused on unconventional gas—including gas shale and tight-gas sand studies—and is the lead scientist for the Western Australian Energy Research Alliance (WA:ERA) Exploration Initiative Scheme (EIS) Tight Gas and Shale Gas research projects. He established Curtin University's Unconventional Gas Research Group in 2010. Reza is the project leader of the Australian National Low Emissions Coal Research and Development's dynamic seal efficiency research project, which is investigating cap rock sealing efficiency for $CO_2$ sequestration in the Gippsland Basin. Reza was also the winner of an Australian Gas Innovation Award 2012 for his innovation on tight gas sand treatment for gas production enhancement.

*R.Rezaee@exchange.curtin.edu.au*

**Milovan Urosevic** of Curtin University's Department of Exploration Geophysics has a PhD in Geophysics. His professional interests are in 3C seismic data processing analysis, 3C Vertical Seismic Profile (VSP) imaging and seismic anisotropy. During his career he has been engaged in several research projects supported by national and international oil and gas companies and these commissions, together with his supervisory work at various universities, have involved a wide range of achievements. He has supervised over 70 MSc and PhD students during his university career to date. He has published more than 80 peer-reviewed journal and conference papers and is the author of one book on Seismic methods.

*M.Urosevic@curtin.edu.au*

**Dr Claudio Delle Piane** works at CSIRO–Earth Science Resource and Engineering and comes from a geological and geomechanical background. He has worked in rock mechanics and rock physics in the rock deformation laboratory at the Swiss Federal Institute of Technology (ETH) in Zurich. He has expertise in experimental rock mechanics testing, scanning electron microscopy and a strong structural geological background.

*Claudio.Dellepiane@csiro.au*